OCTUPOLE CORRELATIONS IN A SYMMETRY CONSERVING FRAMEWORK*

R.N. Bernard[a,b], L.M. Robledo[b], T.R. Rodríguez[b]

[a]CEA, DAM, Île-de-France, 91297 Arpajon, France
[b]Departamento de Física Teórica, Universidad Autónoma de Madrid
28049 Madrid, Spain

(Received December 14, 2016)

Octupole correlations are described in a microscopic framework involving angular momentum, parity and particle number projected intrinsic Hartree–Fock–Bogoliubov states. Linear combinations of those symmetry restored states are considered to account for collective positive and negative parity states in the nucleus ^{144}Ba. The well-known Gogny D1S interaction is used in the calculations. A strong octupole collectivity is observed in the negative parity states justifying the assignment of ^{144}Ba as an octupole deformed nucleus. Higher lying excited states are studied and its structure is identified by looking at the collective wave functions obtained in the calculations. An oblate-spherical 0^+ shape isomer and a two-phonon octupole multiplet are described in detail.

DOI:10.5506/APhysPolB.48.249

1. Introduction

The occurrence of octupole deformation in the ground state of some specific atomic nuclei was predicted long ago (see [1, 2] for reviews). However, it has not been until recently that this prediction has been fully confirmed experimentally [3] thanks to advances in the determination of E3 transition strengths by means of Coulomb excitation experiments with radioactive beams. The reason is that a strong E3 strength is one of the requirements for the existence of permanent octupole deformation in atomic nuclei. The presence of octupole deformation implies the breaking of reflection symmetry in the intrinsic frame, leading to symmetry bands composed of two members of opposite parity in the laboratory frame. Those parity doublets become eventually degenerated in the limit of strong deformation. As the characteristic angular momentum of the octupole excitation is $L = 3$, the dominant

* Presented by L.M. Robledo at the Zakopane Conference on Nuclear Physics "Extremes of the Nuclear Landscape", Zakopane, Poland, August 28–September 4, 2016.

transition between the members of the doublet is of the E3 type although some kind of enhancement on the E1 transitions is expected too. From the theory side, octupole correlations have been studied using an admixture of different techniques including mean field and beyond ones with Skyrme or Gogny interactions [4–11], or methods based on the Interacting Boson Model (IBM) [12–14].

Recent measurements [15] performed in the nucleus ^{144}Ba at the CARIBU facility using the ATLAS accelerator and the CHICO2 and GRETINA detectors have shown that the E3 transition from the 3^- excited state to the ground state is strongly enhanced, signaling thereby the presence of strong octupole correlations (and eventually permanent octupole deformation) in the ground state of this nucleus. From the theory side, the physics of strong octupole correlations in this nucleus was addressed recently [16] using the Hartree–Fock–Bogoliubov (HFB) intrinsic wave functions projected to a good angular momentum, parity and particle number quantum numbers. The axially symmetric quadrupole (Q_2) and octupole (Q_3) moments were used as collective coordinates[1] within the framework of the generator coordinate method (GCM) [17, 18]. The results in this paper show a good agreement with experimental data proving the adequacy of the approach used. The purpose of this paper is to discuss additional results, not presented in [16], like the structure of the collective wave functions of the GCM, the properties of an isomeric oblate 0^+ state obtained in the calculation or the characteristic of two octupole phonon states.

2. Details of the theoretical description

The theoretical description is based on an underlying mean field built with the Gogny D1S energy density functional (EDF) by solving the Hartree–Fock–Bogoliubv (HFB) equation with constraints in the relevant collective degrees of freedom. The HFB intrinsic wave functions are subsequently projected to a good angular momentum, parity and particle number quantum numbers. With those "lab frame" states, linear combinations are made as to obtain the physical states making stationary the energy — see Refs. [17, 18] for a detailed description of all the techniques involved.

2.1. Mean field

The set of intrinsic states $|\varphi(Q_2, Q_3)\rangle$ is obtained by solving the HFB equation with constraints in the $K = 0$ quadrupole Q_{20} and octupole Q_{30} moments and using the Gogny D1S EDF. In the calculation, axial symmetry

[1] In some cases, the dimensionless deformation parameters β_2 and β_3 will be used instead. They are related to the multipole moments of the mass distribution by the general formula $\beta_l = 4\pi\langle r^l Y_{l0}\rangle/(3AR_0^l)$ with $R_0 = 1.2A^{1/3}$ fm.

has been preserved. As a consequence of the breaking of the parity symmetry, a constraint in the center-of-mass coordinate z has to be imposed to keep the center of mass at the origin. The Coulomb interaction is treated exactly by considering both the exchange and pairing channels. This is a requirement to prevent spuriousities associated to the Pauli exclusion principle to leak in the final results. The choice of the D1S parametrization is dictated by its success in reproducing many nuclear properties all over the nuclear chart like. As an example, related to the present study, let us mention the study of octupole correlations all over the periodic table carried out in [10, 19].

2.2. Symmetry restoration

The intrinsic states obtained so far are subsequently projected to a good angular momentum, parity and particle number

$$\left|\Phi^{J,\pi,N,Z}(Q_2,Q_3)\right\rangle = P^J P^\pi P^N P^Z \left|\varphi(Q_2,Q_3)\right\rangle \tag{1}$$

with P^J, P^π, P^N and P^Z being the projectors onto a good angular momentum, parity, neutron number and proton number, respectively [18]. Due to the imposed axial symmetry of the intrinsic states, the traditional projector on a good angular momentum

$$P^J_M = \sum_K g_K P^J_{KM} \tag{2}$$

only gets a contribution from the $K = 0$ term and, therefore, all the overlaps and mean values involving this projector simplify and only require the calculation of an integral in the β Euler angle [20, 21]. Additionally, the restriction to intrinsic states preserving the signature symmetry $\mathcal{S} = \mathcal{P}\mathcal{R}_y(\pi)$ which is composed of the parity operator $\mathcal{P}$ and the rotation of angle π around the y-axis $\mathcal{R}_y(\pi)$ simplifies the projection on a good angular momentum and parity as only those states satisfying the natural parity rule $\pi = (-1)^J$ (even J positive parity, odd J negative one) are allowed [18].

2.3. Configuration mixing

Once the projected intrinsic wave functions $|\Phi^{J,\pi,N,Z}(Q_2,Q_3)\rangle$ are obtained for a relevant range of (discrete) Q_2 and Q_3 values, linear combinations of them are considered

$$\left|\Psi^{J,\pi,N,Z}_\sigma\right\rangle = \sum_{Q_2,Q_3} f^{J,\pi,N,Z}_\sigma(Q_2,Q_3)\left|\Phi^{J,\pi,N,Z}(Q_2,Q_3)\right\rangle \tag{3}$$

by means of a set of amplitudes $f^{J,\pi,N,Z}_\sigma(Q_2,Q_3)$. In the previous expressions, $\sigma = 1,\ldots$ is an index used to label the different linear combinations

(and, therefore, the different final states) with the same J and π values. The amplitudes are determined for each value of the quantum numbers by requiring the energy obtained with the wave functions $|\Psi_\sigma^{J,\pi,N,Z}\rangle$ to be a minimum. This leads to the Hill–Wheeler (HW) equation, and the f amplitudes have to satisfy

$$\sum_{\boldsymbol{q}'} \left(\mathcal{H}^{J\pi}\left(\boldsymbol{q},\boldsymbol{q}'\right) - E_\sigma^{J\pi}\mathcal{N}^{J\pi}\left(\boldsymbol{q},\boldsymbol{q}'\right)\right) f_\sigma^{J\pi}\left(\boldsymbol{q}'\right) = 0\,, \tag{4}$$

where the shorthand notation $\boldsymbol{q} = (Q_2, Q_3)$ has been introduced, and the particle number quantum numbers N and Z have been omitted from the different quantities depending upon them. The quantities entering the HW equation are the norm overlap $\mathcal{N}^{J\pi}(\boldsymbol{q},\boldsymbol{q}') = \langle\Phi^{J\pi}(\boldsymbol{q})|\Phi^{J\pi}(\boldsymbol{q}')\rangle$ and Hamiltonian $\mathcal{H}^{J\pi}(\boldsymbol{q},\boldsymbol{q}') = \langle\Phi^{J\pi}(\boldsymbol{q})|\hat{H}|\Phi^{J\pi}(\boldsymbol{q}')\rangle$ overlap. Given the phenomenological nature of the density-dependent term of the Gogny EDF, a prescription is required for the evaluation of the Hamiltonian overlaps. We use the particle number projected spatial density combined with the mixed prescription for the parity and angular momentum projection. The same mixed prescription is used to compute overlaps between states with different $\boldsymbol{Q}$ and $\boldsymbol{Q}'$ values entering the GCM method. The mixed density prescription avoids the catastrophic behavior of the energy characteristic of prescriptions based on densities preserving spatial symmetries [22]. The impact of the use of the particle number projected density has still to be elucidated.

For each J and π, we obtain a set of different quantum states, which are solution of the HW equation and are characterized by the label σ. The physical interpretation of each of these states is made by looking at a quantity derived from the $f_\sigma^{J\pi}(\boldsymbol{q})$, namely

$$F_\sigma^{J\pi}(\boldsymbol{q}) \equiv \sum_{\boldsymbol{q}'} \left\langle\Phi^{J\pi}(\boldsymbol{q})|\Phi^{J\pi}\left(\boldsymbol{q}'\right)\right\rangle^{1/2} f_\sigma^{J\pi}\left(\boldsymbol{q}'\right) \tag{5}$$

which takes into account the non-orthogonal nature of the generating states $|\Phi^{J,\pi}(\boldsymbol{q}))\rangle$ by means of the square root (in operational sense) of the norm. It turns out that the distribution of the $F_\sigma^{J\pi}(\boldsymbol{q})$ is mostly driven by the potential energy surface obtained by representing the HFB energy as a function of Q_2 and Q_3, and follow the general rules of quantum mechanics: no nodes for the ground state, one node for the first excited state along each degree of freedom, two nodes for the second excited state, one node along Q_2 and another along Q_3, *etc.*

It has to be mentioned that the same technique of combining the GCM with angular momentum, parity and particle number projected wave functions has been applied also with the relativistic mean field [23, 24].

3. Results

Calculations along the lines described above have been carried out for the nucleus ^{144}Ba which was the subject of a recent experiment [15] where a strong E3 transition was measured. This result implies, together with the low excitation energy of the 1^- state, the presence of a permanent octupole deformation in this nucleus. In our study of Ref. [16], we carried out calculations following the procedure described above but focusing our attention to the lowest lying state ($\sigma = 1$) for each possible angular momentum and parity J^π. In this paper, however, we turn our attention to other selected collective excited states corresponding to $\sigma = 2, 3$, *etc.*

As mentioned before, the distribution of the collective amplitudes on the collective variables Q_2 and Q_3 is intimately linked to the structure of the HFB energy as a function of the same variables. This quantity is plotted in Fig. 1 as a function of the deformation parameters β_2 and β_3. As a consequence of the invariance under parity of the underlying nuclear interaction, this quantity is symmetric with respect to the exchange of sign of β_3. The potential energy surface (PES) presents an octupole deformed minimum at $\beta_2 = 0.2$ and $\beta_3 = 0.1$. Its depth is only of 0.90 MeV but this is enough (see below) to concentrate the collective amplitude around the octupole deformed minima. In the same figure, the real shape of the nucleus, in the form of an iso-surface plot, is shown for the configuration corresponding to the HFB minimum. The shape has the characteristic pear shape combined with prolate quadrupole deformation. The two dashed lines represent the self-consistent path along the β_2 (horizontal line) or β_3 (vertical line) degrees

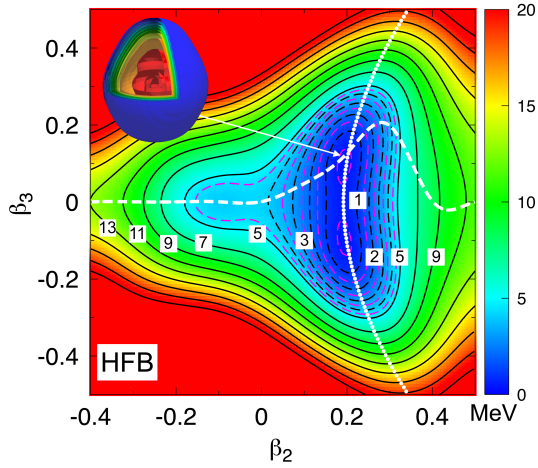

Fig. 1. The HFB energy of the nucleus ^{144}Ba is plotted as a function of the deformation parameters β_2 and β_3 (see the footnote for definition). Also the real spatial density corresponding to the minimum is shown.

of freedom. The latter is the one to be associated with the octupole degree of freedom. The octupole self-consistent path shows a very weak dependence with the quadrupole parameter β_2, typical of a weak quadrupole–octupole coupling (see [16] for a discussion). Finally, let us mention that for $\beta_3 = 0$, there is a rather flat region around $\beta_2 = 0$ that will be of significance in the discussion below.

The solution of the HW equation (Eq. (4)) gives us the energies $E_\sigma^{J\pi}$ and collective amplitudes $f_\sigma^{J\pi}(\boldsymbol{q})$ required to compute the $F_\sigma^{J\pi}(\boldsymbol{q})$ which are the only quantities with the meaning of a probability amplitude. The reason is that the $F_\sigma^{J\pi}(\boldsymbol{q})$ are amplitudes in an orthogonal basis whereas the $f_\sigma^{J\pi}(\boldsymbol{q})$ are not. In order to assign a set of states to a band, we have to look for $F_\sigma^{J\pi}(\boldsymbol{q})$ amplitudes with more or less the same structure as a function of the collective variables. This procedure was followed in [16] to identify both the ground state positive parity rotational band and the negative parity one. In this paper, we are going to study additional structures associated to the amplitudes $|F_\sigma^{J\pi}(\boldsymbol{q})|^2$ depicted in Fig. 2. The amplitude of the 0_1^+ ground state, depicted in Fig. 2, has the typical structure of two Gaussians along each degree of freedom. The width of the Gaussian along the octupole degree of freedom is much larger than the one along the quadrupole direction and extends to be appreciably different from zero at the HFB minimum. It reminds of the square of the ground state wave function of a one-dimensional harmonic oscillator. Negative parity states like the 1_1^-, not shown in the

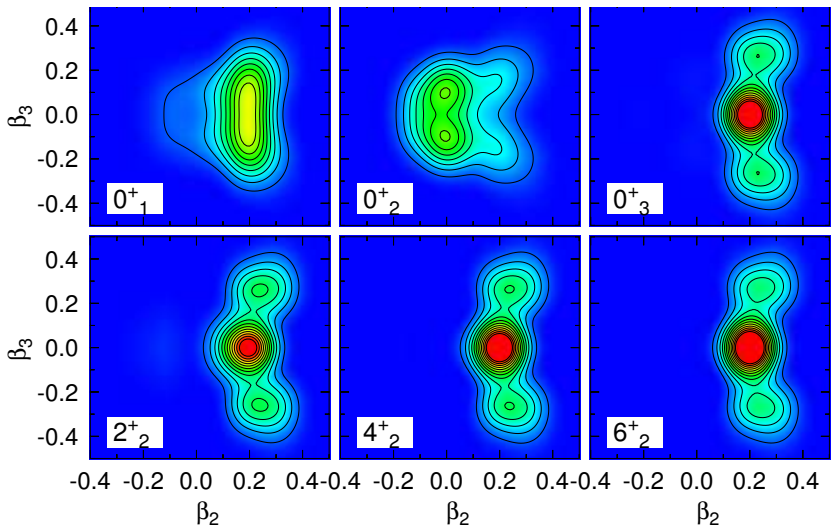

Fig. 2. (Color online) Collective amplitudes $F_\sigma^{J\pi}(\boldsymbol{q})$ of Eq. (5) for different values of J_σ^π are plotted as a function of the deformation parameters β_2 and β_3. The color scale goes from light gray/blue (zero amplitude) to dark gray/red (maximum value of the amplitude).

figure (see [16]), have the shape of a Gaussian along β_2 and two Gaussians (each of them peaked at the two HFB minima) along β_3. It is zero along the $\beta_3 = 0$ line as a consequence of parity symmetry restrictions. The amplitude of the 1^- state reminds the structure of a zero-phonon state along β_2 and a one-phonon state along β_3. In Fig. 2, the amplitude corresponding to the 0_2^+ is shown: it is similar to the one of the ground state (*i.e.* Gaussian shape along both deformation degrees of freedom) but this time centered around $\beta_2 = 0$, a region where the HFB energy is rather flat. This state can be interpreted as an oblate-spherical shape isomer of the ground state and, as discussed below, lies quite low in excitation energy. The next four amplitudes considered in Fig. 2 correspond to the 0_3^+, 2_2^+, 4_2^+ and 6_2^+ states. The four amplitudes look very similar, with three maxima, one at $\beta_3 = 0$ higher that the other two located at $\beta_3 = \pm 0.25$. They correspond to a Gaussian shape along the β_2 degree of freedom (akin to the ground state wave function) and a two-octupole phonon structure along the octupole degree of freedom. We, therefore, conclude that the four states correspond to the multiplet of a two-phonon octupole excitation. As discussed below, the multiplet is not degenerated in energy and the energy centroid is located at an excitation energy higher than twice the energy of a single octupole phonon — the energy of the 3_1^- state. This is a clear indication of the anharmonicity of the octupole excitation and it is no surprising given the octupole deformed character of ^{144}Ba.

The excitation energy of the different states is represented in Fig. 3 in the form of a band-drawing where the states with the same intrinsic structure are assigned to the same band. The positive parity and negative parity rotational bands were already discussed in [16]. The bands turn out to have a much smaller moment of inertia than the experimental one, a characteristic of our calculations related to the fact that only states with $K = 0$ are considered in the calculation [20, 25, 26]. The oblate-spherical isomer discussed above is located at a quite low excitation energy of 1.06 MeV, comparable to the excitation energy of the 3_1^- state at 1.01 MeV. The lowest lying member of the two-octupole phonon multiplet is the 0_3^+ at an excitation energy of 3.03 MeV. The next member is the 2_2^+ at 3.10 MeV, followed by the 4_2^+ at 3.53 MeV and finally the 6_2^+ state at 4.10 MeV. The multiplet is not degenerated in energy with a quite large dispersion in energy of around one MeV. The reason for the splitting as well as the fact that the excitation energy of the multiplet's centroid energy is not located at twice the excitation energy of the 3_1^- is probably the anharmonicity of the excitation and a coupling with the quadrupole degree of freedom. The two-octupole structure was already observed in calculations [11] with the GCM using Q_2 and Q_3 as generating coordinates but without projection to good quantum numbers. In those calculations, more involved structures, like two-phonon quadrupole states or one-phonon quadrupole, one-phonon octupole states were also observed.

The observation of those states in the present calculation requires a larger set of quadrupole and octupole states than the one considered here due to the large spatial extension of the collective amplitudes $F_\sigma^{J\pi}(\boldsymbol{q})$ required to accurately describe those states.

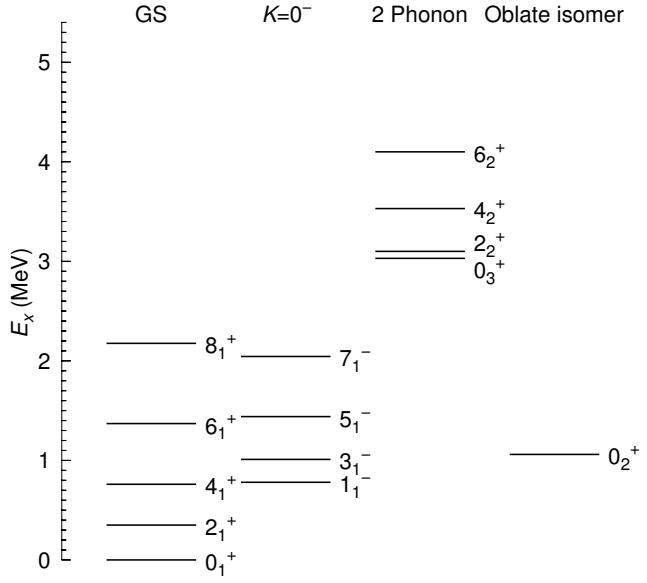

Fig. 3. Theoretical spectrum obtained in the solution of the HW equation. The positive parity rotational band is on the left, followed by the negative parity rotational band. Next is the multiplet corresponding to a two octupole phonon excitation. The last state corresponds to an oblate-spherical shape isomer. No other states with the same structure have been found in our calculation meaning that they are located at a large excitation energy.

As far as we know, neither the oblate-spherical 0_2^+ state nor any of the members of the two-phonon octupole state have been observed experimentally and the results of the present calculation represent a genuine prediction of the method to be confirmed by the experiment.

One of the advantages of the present type of calculations is in the calculation of transition strengths. The wave functions have the proper angular momentum quantum numbers and, therefore, the exact formulas can be used and no approximations like the rotational formula are required [27, 28]. Examples of reduced transition elements are the $|\langle 0_3^+||\mathrm{E3}||3_1^-\rangle| = 0.383\, e\mathrm{b}^{3/2}$ connecting one of the two-phonon octupole states to the one-phonon one. Another reduced matrix element is $|\langle 3_1^+||\mathrm{E3}||6_2^+\rangle| = 0.642\, e\mathrm{b}^{3/2}$ or the $|\langle 2_2^+||\mathrm{E1}||3_1^-\rangle| = 0.016\, e\mathrm{b}^{1/2}$. A thorough analysis of other transitions will be given elsewhere [29].

4. Summary and prospects

We have performed calculations in the framework of the GCM using the quadrupole and octupole degrees of freedom as generating coordinates. Intrinsic wave functions projected to a good angular momentum, parity and particle number are used as basis states. The results obtained with the Gogny D1S interaction for the nucleus ^{144}Ba agree well with recent experimental data. Other higher lying excited states are studied, including an oblate-spherical 0^+ shape isomer and a two-phonon octupole multiplet formed by a 0^+, 2^+, 4^+ and 6^+ state. The proposed method has proven to be flexible enough to describe many low-lying collective excited states of quadrupole and octupole character. An exhaustive study of transition strengths is possible but it is deferred to a future publication. Other issues, as for instance considering other degrees of freedom in the GCM (pairing correlations are a good candidate), will be also addressed in the future.

We acknowledge the support from GSI-Darmstadt and CSC-Loewe-Frankfurt computing facilities. This work was supported in part by the Spanish grants FIS-2014-53434-P MINECO/FEDER, UE, FPA2015-65929-P MINECO/FEDER, UE and FIS2015-63770-P MINECO/FEDER, UE and Programa Ramón y Cajal 2012 No. 11420.

REFERENCES

[1] P.A. Butler, W. Nazarewicz, *Rev. Mod. Phys.* **68**, 349 (1996).
[2] P.A. Butler, *J. Phys. G: Nucl. Part. Phys.* **43**, 73002 (2016).
[3] L.P. Gaffney *et al.*, *Nature* **497**, 199 (2013).
[4] P. Bonche *et al.*, *Phys. Rev. Lett.* **66**, 876 (1991).
[5] J.L. Egido, L.M. Robledo, *Nucl. Phys. A* **524**, 65 (1991).
[6] J.L. Egido, L.M. Robledo, *Nucl. Phys. A* **545**, 589 (1992).
[7] P.-H. Heenen, J. Skalski, P. Bonche, H. Flocard, *Phys. Rev. C* **50**, 802 (1994).
[8] J. Meyer *et al.*, *Nucl. Phys. A* **588**, 597 (1995).
[9] E. Garrote, J.L. Egido, L.M. Robledo, *Phys. Rev. Lett.* **80**, 4398 (1998).
[10] L.M. Robledo, G.F. Bertsch, *Phys. Rev. C* **84**, 054302 (2011).
[11] L.M. Robledo, P.A. Butler, *Phys. Rev. C* **88**, 051302(R) (2013).
[12] J. Engel, F. Iachello, *Nucl. Phys. A* **472**, 61 (1987).
[13] D. Kusnezov, F. Iachello, *Phys. Lett. B* **209**, 420 (1988).
[14] K. Nomura, R. Rodríguez-Guzmán, L.M. Robledo, *Phys. Rev. C* **92**, 014312 (2015).
[15] B. Bucher *et al.*, *Phys. Rev. Lett.* **116**, 112503 (2016).

[16] R.N. Bernard, L.M. Robledo, T.R. Rodríguez, *Phys. Rev. C* **93**, 061302 (2016).

[17] M. Bender, P.-H. Heenen, P.-G. Reinhard, *Rev. Mod. Phys.* **75**, 121 (2003).

[18] P. Ring, P. Schuck, *The Nuclear Many Body Problem*, Springer-Verlag, Berlin 1980.

[19] L.M. Robledo, *J. Phys. G: Nucl. Part. Phys.* **42**, 055109 (2015).

[20] R.R. Rodríguez-Guzmán, J.L. Egido, L.M. Robledo, *Phys. Rev. C* **62**, 054319 (2000).

[21] R. Rodríguez-Guzmán, J.L. Egido, L.M. Robledo, *Nucl. Phys. A* **709**, 201 (2002).

[22] L.M. Robledo, *J. Phys. G: Nucl. Part. Phys.* **37**, 064020 (2010).

[23] J.M. Yao, E.F. Zhou, Z.P. Li, *Phys. Rev. C* **92**, 041304 (2015).

[24] E.F. Zhou *et al.*, *Phys. Lett. B* **753**, 227 (2016).

[25] M. Borrajo, T.R. Rodríguez, J.L. Egido, *Phys. Lett. B* **746**, 341 (2015).

[26] J.L. Egido, M. Borrajo, T.R. Rodríguez, *Phys. Rev. Lett.* **116**, 052502 (2016).

[27] J.L. Egido, L.M. Robledo, Y. Sun, *Nucl Phys. A* **560**, 253 (1993).

[28] L.M. Robledo, G.F. Bertsch, *Phys. Rev. C* **86**, 054306 (2012).

[29] R.N. Bernard, L.M. Robledo, T.R. Rodriguez, in preparation.